JACS
JOURNAL OF THE AMERICAN CHEMICAL SOCIETY
Article
pubs.acs.org/JACS

Binding Modes of Carboxylate- and Acetylacetonate-Linked Chromophores to Homodisperse Polyoxotitanate Nanoclusters

Jesse D. Sokolow,[†] Elzbieta Trzop,[†] Yang Chen,[†] Jiji Tang,[†] Laura J. Allen,[‡] Robert H. Crabtree,[‡] Jason B. Benedict,*[,†] and Philip Coppens*[,†]

[†]Chemistry Department, University at Buffalo, SUNY, Buffalo, New York 14260-3000, United States
[‡]Department of Chemistry, Yale University, New Haven, Connecticut 06520-8107, United States

Supporting Information

ABSTRACT: The binding of carboxylate- and acetylacetonate-linked chromophores to homodisperse polyoxotitanate nanoclusters with 17 Ti atoms or more are surveyed and found to be limited to chelate-bidentate and the bridging modes, the former being dominant for the acetylacetonate-linked chromophores, the latter for the carboxylate linkers. Chromophores with acetylacetonate linking groups invariably bind in the chelate mode, whereas carboxylic acid terminated chromophores more frequently are observed to have the bridging mode, with the exception of three cases in which a strong electron-donating substituent is present on two different sensitizers. The calculations for isonicotinateand nitrophenylacetylacetonate functionalized Ti17 clusters show the observed binding modes to correspond to the lower energy functionalized clusters, but do not predict the difference between the cinnamic acid and dimethylaminocinnamic acid binding to Ti17, which are bridging and chelate respectively. Both binding modes were never observed to occur for a single chromophore, even when synthetic conditions were varied. Density of state calculations show broadening and splitting of the chromophore LUMO on complexation due to interaction with the cluster's conduction band, as well as frequent penetration of sensitizer orbitals into the bandgap of the functionalized nanoparticle.

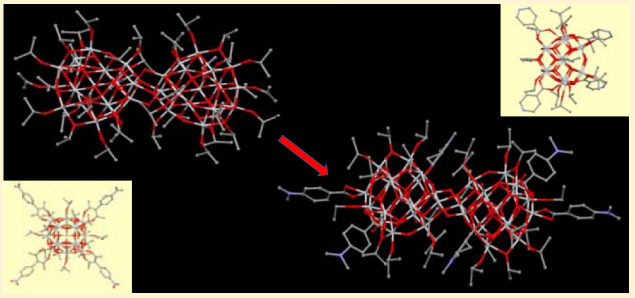

1. INTRODUCTION

Photoinduced electron injection from sensitizers to semiconductor substrates is a key component of photovoltaic cells, and dependent on the mode of attachment of the chromophores and the structure of the layer to which they are attached. Notwithstanding extensive theoretical and experimental studies on the mechanism of photoinduced electron injection into anatase semiconductor surfaces typical for TiO-based photovoltaic cells, little precise information on the binding modes of the sensitizers to the anatase surfaces has been available. The lack of structural information has necessitated the use of varying assumptions in theoretical calculations,[1−3] or theoretical optimization to derive information on the binding modes.[4−7] However, relevant experimental information can now be obtained by X-ray diffraction studies of crystalline arrangements of functionalized homodisperse polyoxotitanate clusters,[8,9] which are suitable model compounds for this purpose. Their structures have features typical for the TiO polymorphs anatase and brookite, but also show distortions more likely to occur in surface layers of the bulk compounds.

In this paper we report the binding modes, as precisely determined by X-ray diffraction, of a number of carboxylate- and acetylacetonate-linked photosensitizers attached to polyoxotitanate particles with nuclearities of 17−34 titanium atoms. Acetylacetonate has been proposed as a particularly robust linker under aqueous and oxidative conditions.[10] As a result of the synthetic route the clusters are capped by alkoxide substituents which prevent agglomeration. We present parallel theoretical calculations, based on the new experimental structural information, to quantify the energy differences between different modes of attachment and examine changes in the density of states on functionalization.

We note that in a series of recent papers Rustad and coworkers have emphasized the need to understand the surface coordination environment to explain the rates and mechanism of reactions occurring at the surface of oxide materials and have performed theoretical calculations on polyoxometalate nanoparticles to obtain such information.[11−13] The combined experimental-structure/theoretical approach described below should be similarly applicable to a wide range of such systems.

2. CLASSIFICATION OF BINDING MODES

Ti/O nanoclusters up to Ti_{28} have been reviewed in detail by Rozes and Sanchez,[14] whereas the binding modes of Ti-oxide clusters with up to 10 Ti atoms with catechol, salicylic acid, and 2,2′-biphenol have been surveyed by Gigant et al.[15] For catechol and salicylic acid, which have two linking oxygen atoms, like the chromophores discussed in this article, five essentially different

Received: April 17, 2012
Published: June 19, 2012

   dx.doi.org/10.1021/ja303692r | J. Am. Chem. Soc. 2012, 134, 11695−11700

binding modes are observed in the smaller clusters: (a) monodentate μ_1-(O); (b) chelate-bidentate μ_1-(O,O); (c) bridging μ_2-(O,O′); (d) bridging chelate μ_2-(O,O′,O′); and (e) doubly bridging chelate μ_3-(O,O′,O,O′), in which the ′ signals binding to a different Ti atom. These modes are illustrated in Scheme 1 for the case of catechol. Whereas all five are observed

Scheme 1. Summary of Chromophore Binding Modes

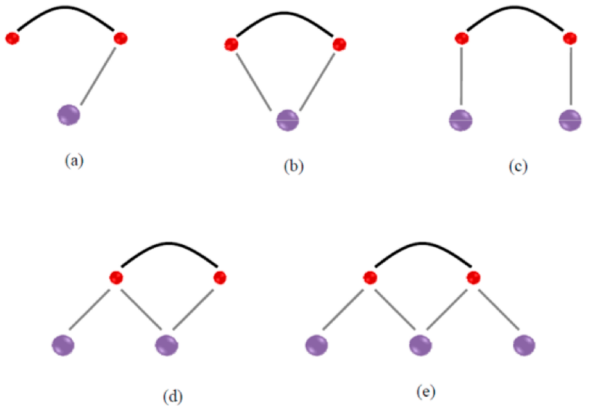

in the smaller clusters, the binding is less variable in clusters with more than 10 titanium atoms, for which only (b) and (c), chelate-bidentate μ_1-(O,O) and the bridging μ_2-(O,O′) modes respectively have been observed.

Table 1 lists the polyoxotitanate clusters with 17 or more Ti atoms discussed here. All are terminated with alkoxides in the nonfunctionalized sites. The chromophores examined are illustrated in Scheme 2.

3. THE STRUCTURE OF THE T17 CLUSTERS

The crystallographic symmetry of the Ti17 cluster in the structures examined varies from none, i.e. 1, to 2, m to $\bar{4}$, with the number of molecules or molecular fragments in the asymmetric unit varying from 2 to 1 to 1/2 to 1/4 (Table 1). The crystallographic symmetry is strongly affected by the molecular packing in the crystal, which for the functionalized

Scheme 2. Molecular Diagrams of the Sensitizer Molecules

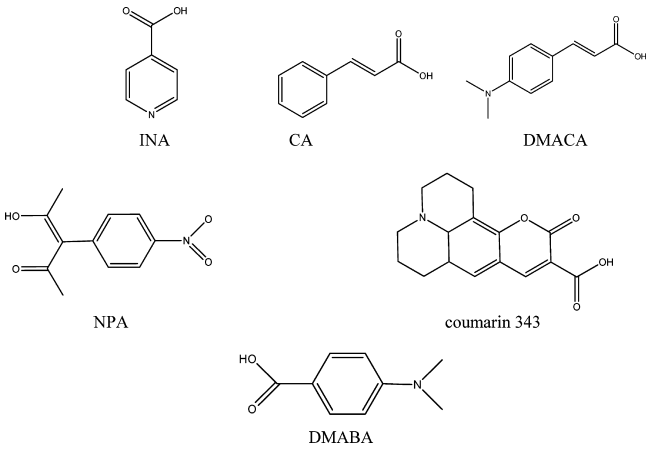

clusters is dominated by interaction between the attached chromophores through, for example, $\pi-\pi$-stacking. The variation in crystallographic symmetry of the nanoclusters is demonstrated by the two known polymorphs of the non-sensitized Ti17 cluster. One of these crystallizes in the space group $P2_1/c$, common for molecular crystals, with one molecule in the asymmetric unit, i.e. Z′ = 1, while the second polymorph occupies a 2-fold axis of the space group $C2/c$. Similar differences occur in the structures of the sensitized clusters. Nevertheless, close examination shows that not only the connectivity but also the detailed molecular structures of all Ti17 clusters are remarkably similar, as illustrated in Figure 1, with the local point group symmetry being very close to $\bar{4}$ in all cases.

4. SURVEY OF BINDING MODES OF THE CHROMOPHORES

As is evident from examination of Table 1, the variety of binding modes is severely restricted in the larger clusters, only two of the five binding modes identified by Gigant et al.[15] being observed. This sharply differs from the binding modes observed

Table 1. TiO/Chromophore Clusters with 17−34 Ti Atoms (90 K unless Marked Otherwise)[a]

	color	no. of ligands	Binding mode	mol. symm.	Z′, space group	ref/CCSD code
Ti17 (200 K)	colorless	–	–	1	1, $P2_1/c$	9, 16, LIDJUD
Ti17	colorless	–	–	2	1/2, $C2/c$	[b]
			Acid Linkers			
Ti17-t-CA (200 K)	colorless	2	bridging (O,O′)	2	1/2, $C2/c$	[b]
Ti17-t-DMACA	yellow	4	bidentate (O,O)	m	1/2, $P2_1/m$	[b]
Ti17-DMABA	yellow	4	bidentate (O,O)	$\bar{4}$	1/4, $I4_1/a$	[b]
Ti17-INA	colorless	4	bridging (O,O′)	$\bar{4}$	1/4, $I4_1/a$	[b]
Ti18-acetic acid	colorless	10	bridging,(O,O′)	1	1, $P\bar{1}$	8, OPUQIA
Ti18-propionic acid	colorless	10	bridging,(O,O′)	1	1, $P\bar{1}$	[b]
Ti28-acetic acid	colorless	12	bridging (O,O′)	$\bar{2}$	1/2, $R\bar{3}c$	8, OPUQOG
Ti34-DMABA	pale-yellow	6	bidentate (O,O)	$\bar{1}$	1/2, $P\bar{1}$	[b]
			Acetylacetonate-Type Linkers			
Ti17-acac	colorless	4	bidentate (O,O)	m	1/2, $Pnma$	[b]
Ti17-NPA	pale-yellow	4	bidentate (O,O)	2	1/2, $C2/c$	[b]
Ti17-APA	pale-yellow	4	bidentate (O,O)	1	1, $P\bar{1}$	[b]
Ti17-coumarin-343	orange	2	bidentate	$\bar{2}$	1/2, $C2/c$	[b]
Ti18-acac	colorless	2	bidentate (O,O)	$\bar{1}$	1, $P\bar{1}$	17

[a]Abbreviations: APA, 4-aminophenylacetonate; CA, *trans*-cinnamate; DMACA, 4-dimethylamino *trans*-cinnamate; DMABA, dimethylamino benzoate; INA, isonicotinate; NPA, nitrophenyl acetylacetonate. [b]This work.

dx.doi.org/10.1021/ja303692r | J. Am. Chem. Soc. 2012, 134, 11695−11700

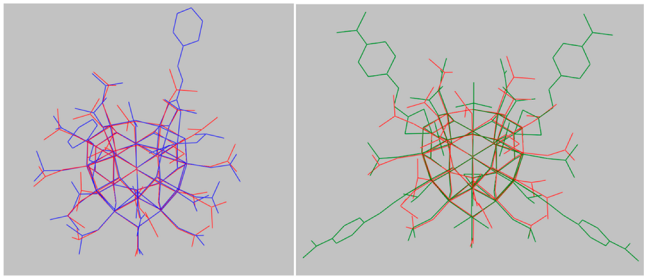

Figure 1. Overlay of the unsubstituted Ti17 cluster (red) with (a) the bridging bis-cinnamic acid (CA) complex (blue) and (b) the tetra-dimethylaminocinnamic acid complex (DMACA) (green). The local −4 axes of the TiO clusters are vertical in the drawing and pass through the 4-coordinate central Ti atom.

in the smaller clusters in which all five types occur. In the smaller clusters the Ti atoms are often accessible from several directions, as in $Ti_6(\mu_3\text{-}O)(cat)_6(OPri)_{10}$, in which one of the Ti atoms is seven-coordinate.[9]

In the larger clusters, the predominant binding mode tends to be bridging for the carboxylic acid linkers with the exception of the DMABA substituent in both Ti17 and Ti34 and DMACA in Ti17, suggesting a decisive influence of the electron-donating dimethylamino substituent which is also evident in the calculated density of states discussed in section 6. In contrast, the acetylacetonate linker is invariably observed to be chelating-bidentate. It is of interest that this occurs even though O---O bite distance is larger in acetylacetonate than in the carboxylic acids (Table S1). Favorable overlap between the oxygen-p and Ti-d orbitals in this geometry may be a contributing factor.

In the bidentate mode the substituent replaces an alkoxide ligand attached to a 5-coordinate Ti, which becomes 6-coordinate; in the bridging mode linking occurs to one 5-coordinate and one 6-coordinate site, at the latter the substituent replaces an alkoxide ligand such that the Ti coordination remains 6-fold as illustrated in Figure 2, and analyzed further in section 5.

Both anchoring modes are compatible with the conclusion reached by Chen et al. based on Ti K-edge XANES of ∼19 Å nanoparticles that a pentacoordinate Ti geometry at the surface of the nanoparticles is restored to six-coordinate on functionalization.[18]

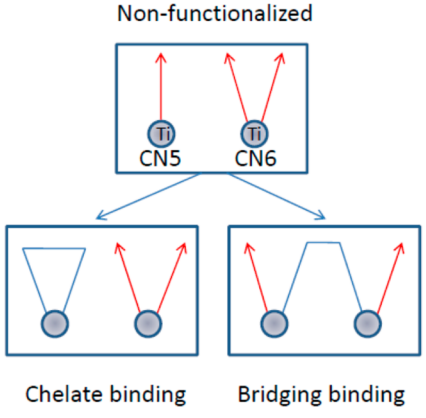

Figure 2. Schematic representation of the functionalization reaction. Red arrows represent the alkoxide ligands, blue lines the attached chromophores.

In principle two different bridging modes can occur. The 5-coordinate Ti is participating in four Ti−O−Ti−O rhombic arrangements, two of which have Ti−Ti distances of ∼2.95 Å, while the distances are ∼3.01 Å in the other two rhombs. The observed arrangement in all cases corresponds to bridging of the longer Ti−Ti distance, which we will refer to here as bridging mode 1. The difference is illustrated in Figure 3. Results of energy calculations for both modes are included in Tables 2 and 3.

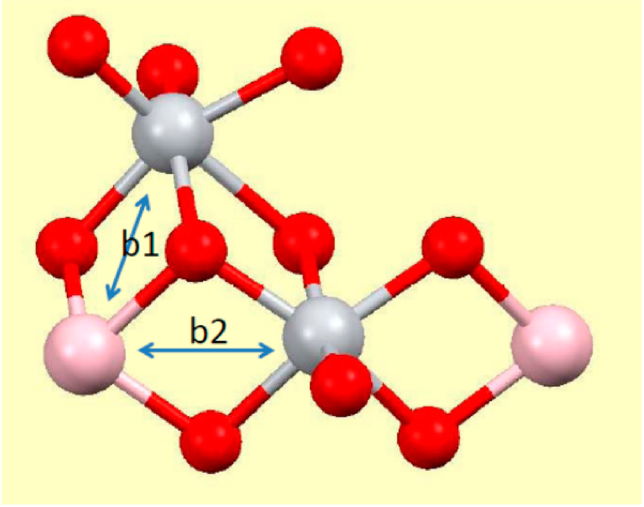

Figure 3. Fragment of the Ti17 cluster indicating the two alternative bridging modes, 5-coordinate Ti atoms colored purple. Mode 1, atoms linked by the canted arrow are bridged; mode 2, atoms linked by the horizontal arrow are bridged. Only mode 1 has been observed in the experimental structures.

Ti18 and Ti28 have the largest adsorbate to Ti ratio in the samples studied of 10/18 (0.556) and 12/28 (0.429) respectively, both with the small acetate or propionate substituents, vs maximally 4/17 (0.235) in Ti17 and 6/34 (0.176) in Ti34. In the known functionalized structures of Ti18 and Ti28 two Ti's are bridged by acetate or propionate ions. The larger ratios have so far only been observed for the small nonchromophoric adsorbates. They are not included in following discussion of the sensitizer-cluster bonding. Chromophore-cluster interatomic distances in the linking regions are summarized in Table S1.

5. THEORETICAL ANALYSIS OF THE BINDING MODES

Method. None of our experiments revealed alternate binding modes for the same chromophore-cluster combination, nor did different clusters bind any one chromophore in different ways. Thus, the binding is highly specific. We have investigated the absence of duplicate binding modes of the same chromophore by computer-modeling Ti17 clusters with isonicotinic acid (INA) and nitrophenyl acetylacetonate (NPA) in the alternate binding modes. As the Ti17 clusters' geometry showed remarkable constancy independent of the crystal symmetry or substitution, as described above, we have retained the −4 (S4) symmetry of, among others, the INA and dimethylaminocinnamic acid (DMACA) Ti17 structures, which show bridging and bidentate binding respectively (Table 1), thereby greatly reducing the computational complexity.

dx.doi.org/10.1021/ja303692r | J. Am. Chem. Soc. 2012, 134, 11695−11700

Table 2. Results of the Geometry Optimizations for Methoxide-Substituted Cluster[a]

	calculations			experiment		
	Ti−O distances			Ti−O distances		
	5-coord	6-coord	O−O distance in ligand	5-coord	6-coord	O−O distance in ligand
INA_bridging-1	2.242	2.006	2.280	2.198	1.968	2.276
INA_bidentate	2.138, 2.185	–	2.208	–	–	–
INA_bridging-2	2.291	1.939	2.279	–	–	–
NPA_bridging-1	2.137	1.948	2.802	–	–	–
NPA_bidentate	2.080, 2.021	–	2.568	2.020, 2.030, 2.050, 2.015	–	2.594, 2.591
CA_bridging-1	2.238	1993	2.286	2.269	1.961	2.284
CA_bidentate	2.155, 2.118	–	2.208	–	–	–
DMACA_bidentate	2.121, 2.136	–	2.208	2.108, 2.066, 2.095, 2.064	–	2.181, 2.155
DMACA_bridging-1	2.200	1.986	2.287	–	–	–

[a]The site labeled 5-coord is 5-coordinate before substitution, but 6-coordinate after substitution has taken place.

Table 3. Final Total Energies (Hartrees) for the Optimized Isonicotinic Acid (INA), Nitrophenyl Acetylacetonate (NPA), and Dimethylaminocinnamic Acid (DMACA) Binding Modes of the $Ti_{17}O$ Cluster

calculations	isopropoxide	delta[a]	methoxide	delta[a]
INA_bridging-1	−21093.705	0	−19835.787	0
INA_bidentate	−21093.587	0.118	−19835.677	0.110
INA_bridging-2	−21093.615	0.090	−19835.723	0.064
NPA_bridging-1	−22471.191	0.019	−21213.303	−0.014
NPA_bidentate	−22471.210	0	−21213.317	0
CA_bridging-1	−20731.555	0	−19316.401	0
CA_bidentate	−20731.499	0.056	−19316.348	0.054
DMACA_bridging-1	−21874.915	0	−20616.995	0
DMACA_bidentate	−21874.805	0.109	−20616.896	0.099

[a]difference with the lowest energy binding mode.

Double-zeta 6-31G B3LYP calculations were used with the Gaussian09 software.[19] The Ti−O core was fixed at the crystallographically determined geometry, but the chromophore, including the bridging oxygen atoms, and the alkoxide ligands were allowed to adjust in the geometry optimization. To examine the effect of the nature of the alkoxide ligands, optimizations were performed both with the isopropoxide and the smaller methoxide ligands. Three binding modes were examined, the chelate (bidentate) mode and the two alternative bridging modes, bridging-1 and bridging-2, illustrated in Figure 2. Only the first of these has been observed in the crystallographic analyses. Frequency calculations were performed for the optimized fragments of several of the final structures to ensure that an equilibrium conformation with no imaginary frequencies had been reached.

Results. Results of the calculations are summarized in Tables 2 and 3. Table 2 shows both the theoretical and experimental geometries (where available) for the isopropoxide-substituted functionalized clusters, whereas total energies for both the isopropoxide- and methoxide-covered functionalized clusters are listed in Table 3.

As may be expected, the experimental geometries in the binding region are not exactly reproduced by the calculations, although the agreement is typically within a few hundreds of an Å. The asymmetry in the bridging 1 mode is almost in quantitative agreement with the observed dimensions in the INA functionalized complex, with the bond to the former 5-coordinate site being longer by almost 0.25 Å. The chelate binding in the NPA complex is slightly asymmetric in agreement with one, but not the other independent binding site observed experimentally. The experimental energies predict the bridging-1 mode to be most stable in the INA complex by 0.118 H in agreement with the observed geometry, and less stable for NPA by 0.019 H, again in agreement with the crystallographic result. The nonobserved bridging-2 mode of INA is predicted to be less stable than the observed bridging-1. The ranking is not affected by the substitution of methoxide for isopropoxide, illustrating the passive nature of the alkoxide substituents. The observed bridging-1 mode is also predicted to be more stable than the chelating mode for cinnamic acid (CA). However, this is not the case for 4-dimethylaminocinnamic acid (DMACA), which unexpectedly is observed to bind differently from CA (Table 1). This energy discrepancy between the theory used and experiment remains unexplained, although differences in the band structure are evident, as described in the following section.

6. DENSITY OF STATES OF TI17 CLUSTERS BEFORE AND AFTER FUNCTIONALIZATION

Density of states (DOS) plots for INA, NPA, CA, and DMACA for both the chelate-bidentate and the bridging geometries were calculated with a 6-31G basis set, B3LYP functional using Gaussian09. They are reproduced in Figure 4 together with the diagram of the unfunctionalized cluster and the free chromophore. A dominant feature observed in all diagrams is the broadening and splitting of the chromophore LUMO on complexation due to overlap with the cluster orbitals, a feature often associated with efficient electron transfer.[1,20] The difference between cinnamic acid (CA, bridging, 2 attached chromophores) and dimethylaminocinnamic acid (DMACA, chelate-bidentate, 4 attached chromophores) is typified by the HOMO of the sensitizer, with its large dimethylamino (DMA) contribution, being located in the bandgap and a large smearing of the LUMO in the observed DMACA chelate mode, indicating improved electron-donating properties of the DMA substituted cinnamic acid.

There is a clear change between the alkoxide DOS, shown in purple in Figure 4, of the chelate and bridging models. In the latter the highest energy peaks disappear and shift to lower energies compared with the chelating structures in which the single alkoxide ligand on the formerly 5-coordinate Ti is removed, rather than one of the two ligands on the 6-coordinate Ti (Figure 2). The latter binding mode of the alkoxides is apparently energetically more favorable.

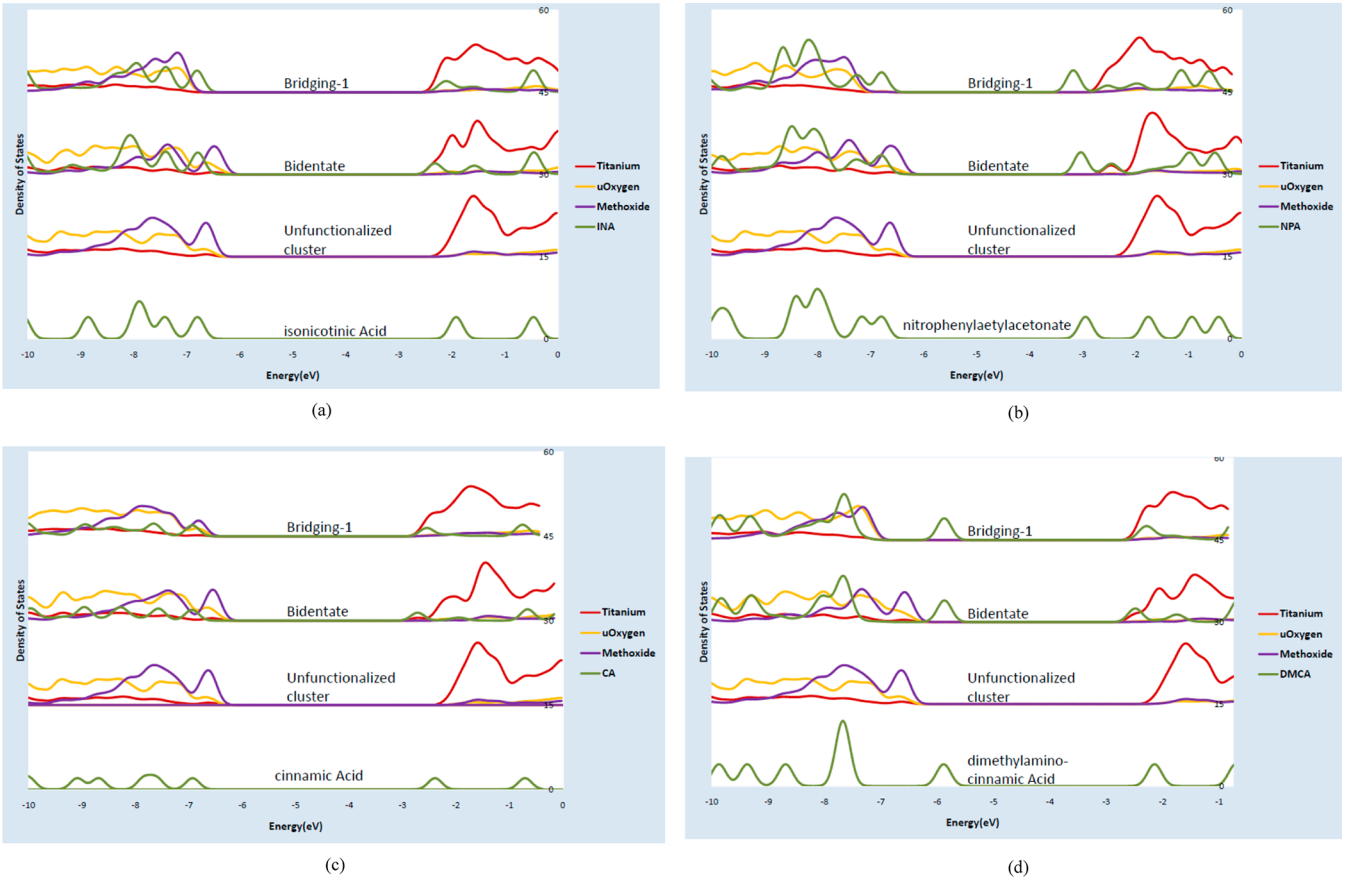

Figure 4. Calculated density of states of functionalized Ti17 clusters: (a) isonicotinic acid (INA), observed bridging; (b) nitrophenyl acetylacetonate (NPA), observed chelate-bidentate; (c) cinnamic acid (CA), bridging; and (d) dimethylaminocinnamic acid, observed chelate-bidentate.

7. CONCLUSIONS

The chromophore binding modes in the nanoclusters with 17 Ti atoms or more, reported above, are limited to the chelate (bidentate) and the bridging modes. In both cases a titanium atom that is 5-coordinate before chromophore binding participates. In the bridging mode the second bond is to an initially 6-coordinate Ti, which loses an alkoxide ligand on functionalization. Of the two possible bridging modes the one involving a second Ti not linked by oxygen bridges to a second 5-coordinate Ti ("bridging-1") is observed. Chromophores with acetylacetonate linking groups invariably bind in the chelate mode, whereas carboxylic acid terminated sensitizers more frequently bind in the bridging mode, except in the two cases in which an electron donating substituent is introduced. The energy calculations for INA and NPA functionalized Ti17 clusters show the observed binding modes to correspond to the lower energy clusters. However they do not explain the difference between the cinnamic acid and dimethylaminocinnamic acid binding, the former being bridging, whereas the latter is observed to be chelate, although the calculated band structures differ significantly. The homodisperse small clusters reported here have a large surface area and thus may be more typical for surface layers than for the Ti/O semiconductor bulk structure.

■ ASSOCIATED CONTENT

Supporting Information

Interatomic distances in the linking region of the clusters, synthetic procedures, and CIF files. This material is available free of charge via the Internet at http://pubs.acs.org.

■ AUTHOR INFORMATION

Corresponding Author

coppens@buffalo.edu; jbb6@buffalo.edu

Notes

The authors declare no competing financial interest.

■ ACKNOWLEDGMENTS

This work was funded by the Division of Chemical Sciences, Geosciences, and Biosciences, Office of Basic Energy Sciences of the U.S. Department of Energy through Grant DE-FG02-02ER15372.

■ REFERENCES

(1) Persson, P.; Lundqvist, M. J.; Ernstorfer, R.; Goddard, W. A.; Willig, F. *J. Chem. Theory Comput.* **2006**, *2*, 441.
(2) Wolpher, H.; Sinha, S.; Pan, J.; Johansson, A.; Lundqvist, M. J.; Persson, P.; Lomoth, R.; Bergquist, J.; Sun, L.; Sundstrom, V.; Akermark, B.; Polivka, T. *Inorg. Chem.* **2007**, *46*, 638.
(3) Sheka, E. F.; Zayets, V. A. *Phys. Solid State* **2007**, *49*, 2004.
(4) Vittadini, A.; Selloni, A.; Rotzinger, F. P.; Gratzel, M. *J. Phys. Chem. B* **2000**, *104*, 1300.
(5) Redfern, P. C.; Zapol, P.; Curtiss, L. A.; Rajh, T.; Thurnauer, M. C. *J. Phys. Chem. B* **2003**, *107*, 11419.

(6) Nilsing, M.; Lunell, S.; Persson, P.; Ojamäe, L. *Surf. Sci.* **2005**, *582*, 49.
(7) Nilsing, M.; Persson, P.; Ojamäe, L. *Chem. Phys. Lett.* **2005**, *415*, 375.
(8) Benedict, J. B.; Freindorf, R.; Trzop, E.; Cogswell, J.; Coppens, P. *J. Am. Chem. Soc.* **2010**, *132*, 13669.
(9) Benedict, J. B.; Coppens, P. *J. Am. Chem. Soc.* **2010**, *132*, 2938.
(10) McNamara, W. R.; Snoeberger, R. C.; Li, G. H.; Schleicher, J. M.; Cady, C. W.; Poyatos, M.; Schmuttenmaer, C. A.; Crabtree, R. H.; Brudvig, G. W.; Batista, V. S. *J. Am. Chem. Soc.* **2008**, *130*, 14329.
(11) Ohlin, C. A.; Villa, E. M.; Rustad, J. R.; Casey, W. H. *Nat. Mater.* **2010**, *9*, 11.
(12) Rustad, J. R.; Casey, W. H. *Nat. Mater.* **2012**, *11*, 223.
(13) Wang, J. W.; Rustad, J. R.; Casey, W. H. *Inorg. Chem.* **2007**, *46*, 2962.
(14) Rozes, L.; Sanchez, C. *Chem. Soc. Rev.* **2011**, *40*, 1006.
(15) Gigant, K.; Rammal, A.; Henry, M. *J. Am. Chem. Soc.* **2001**, *123*, 11632.
(16) Steunou, N.; Kickelbick, G.; Boubekeur, K.; Sanchez, C. *J. Chem. Soc., Dalton Trans.* **1999**, 3653.
(17) Toledano, P.; In, M.; Sanchez, C. *C.R. Acad. Sci. Paris* **1991**, *313*, 1247.
(18) Chen, L. X.; Rajh, T.; Jager, W.; Nedeljkovic, J.; Thurnauer, M. C. *J. Synchrotron Rad.* **1999**, *6*, 445.
(19) Frisch, M. J. et al., *Gaussian09*, Revision A.1; Gaussian Inc.: Pittsburgh, PA, 2009.
(20) Lundqvist, M. J.; Nilsing, M.; Persson, P.; Lunell, S. *Int. J. Quantum Chem.* **2006**, *106*, 3214.